

THE BEAM TRAJECTORY MONITOR FOR THE TTF-FEL AT DESY

S. Hillert, II. Institut für Experimentalphysik, Universität Hamburg, Hamburg, Germany
P. Holl, P. Lechner, KETEK GmbH, Oberschleißheim, Germany
R. Ischebeck, S. Karstensen, U.C. Müller, J.S.T. Ng, S. Roth, DESY, Hamburg, Germany
G. Petzold, AB Halbleitertechnologie, TU Hamburg-Harburg, Germany
H. Thom, DESY, Zeuthen, Germany

Abstract

The design, construction and first tests of a prototype of the beam trajectory monitor at the TTF-FEL are presented. With this monitor the off-axis spontaneous undulator radiation is imaged through a set of pinholes onto silicon pixel detectors. This allows to measure simultaneously 12 points of the transverse beam position with an accuracy of better than $10\ \mu\text{m}$ over a length of 5 m. The prototype consists of a pinhole mask and the pixel detectors accurately placed to each other inside a vacuum chamber which is held under beam vacuum. We first present the design and the production technology of the silicon pixel detector. Then the optimization of the pinhole mask and its realization using lithographic methods are discussed. To determine its spatial accuracy the detector is scanned using a laser test stand and a low-intensity electron beam of an electron microscope. The symmetry axis of the detector defines a straight line within $0.4\ \mu\text{m}$. Additionally, the electron microscope is used to study the radiation hardness of the detector. The sensitivity of the detector to low energy X-rays is measured using a vacuum ultraviolet beam at the synchrotron light source HASYLAB. Finally first calibration measurements of the BTM prototype detectors are shown.

1 DESIGN AND CONSTRUCTION OF THE BTM PROTOTYPE

1.1 Measurement Principle

In order to achieve the high brightness promised by the single-pass Free Electron Laser (FEL) at the TESLA Test Facility (TTF) [1], the electron beam position must be controlled to better than $10\ \mu\text{m}$ over the 15 m long undulator. With the beam trajectory monitor (BTM) [2] the off-axis spontaneous undulator radiation is imaged through a set of pinholes (see Fig. 1). A silver foil across each pinhole

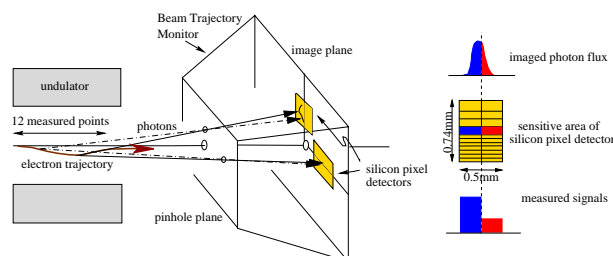


Figure 1: Measurement principle of the BTM.

absorbs all low energy photons and restricts the spectral range of the detected radiation to energies above 100 eV. To achieve the required resolution of the BTM, the center of the photon spot will be measured with a precision of better than $1\ \mu\text{m}$ using high resolution silicon pixel detectors.

1.2 The Silicon Pixel Detector

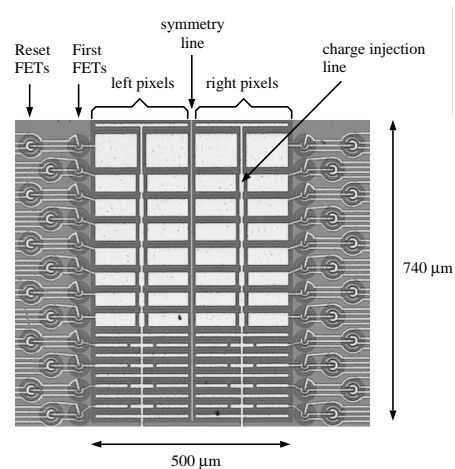


Figure 2: The silicon pixel detector.

A silicon pixel detector with an active area of $0.5\ \text{mm} \times 0.74\ \text{mm}$ and a total of 24 channels was designed and fabricated at the MPI Halbleitertechnologie. The sensitive area of the detector consists of two rows of each 12 active pixels as shown in Fig. 2. The pixels are $250\ \mu\text{m}$ wide, with heights varying from $25\ \mu\text{m}$ (nearest to beam) to $100\ \mu\text{m}$ to give roughly equidistant measuring points in the projection along the undulator axis. Detailed calculation and simulations which determine the present design and realization of the BTM pixel detector can be found in [2].

The concept of a backside illuminated pn -junction detector has been chosen, which shows not only a high quantum efficiency for the desired photon energies, but in addition an excellent spatial homogeneity [3]. It consists of a fully depleted n -type bulk and a non structured p^+ -rear contact, acting as radiation entrance window. Applying a negative voltage of about 120 V to the rear contact totally depletes the detector and causes the signal electrons to drift towards the collecting n^+ pixel anodes. High quantum efficiency is achieved using a thin entrance window technology.

The pixels are formed by n^+ -implants and are isolated from each other by a $5\ \mu\text{m}$ wide p^+ grid. Each pixel anode is connected to an amplifying JFET which is integrated on the detector chip, thus minimizing stray capacitances. The $4\ \text{mm} \times 2.5\ \text{mm}$ large detector chips are mounted onto a ceramic hybrid board. Each detector pixel is connected to one channel of the CAMEX64B read-out chip. It provides signal amplification, base line subtraction, and multiplexed output.

1.3 The Pinholes

The BTM uses a set of pinholes to project an image of the electron beam onto the silicon pixel detector. The pinholes are placed at a distance of $4.5\ \text{mm}$ from the beam axis. Maximum resolution is achieved with minimum photon spot size on the detector plane. In order to reduce the effect of diffraction, only the higher harmonics of the spontaneous undulator radiation will be used for BTM measurements. This is achieved by putting a silver foil across the pinhole which absorbs the photons with energies below $100\ \text{eV}$. Numerical methods have been used to simulate the diffraction pattern of the pinhole at the place of the detector. For the given spectral range, an optimum pinhole diameter of $80\ \mu\text{m}$ has been found which minimizes the photon spot size.

The only way to produce apertures or diaphragms with structure details smaller than $100\ \mu\text{m}$ is electro-plating in combination with a photolithographically structured form. This method is well known from the LIGA¹ technology. Gold is chosen as electro-plating material since it is non magnetic and can be readily electro-plated.

Silver foils are put across each pair of horizontal and vertical pinhole. One pair is supplied with a $120\ \text{nm}$, the other with a $240\ \text{nm}$ thick foil.

1.4 The Vacuum Chamber

A total view of the prototype monitor is shown in Fig. 3. It consists of a vacuum chamber kept under beam vacuum and mounted onto a precise adjustment table. The pinhole mask and the detector hybrid are attached to both sides of a $520\ \text{mm}$ long aluminum cylinder which is precisely implemented into the supporting vacuum chamber.

Exact alignment of the detector chips and the pinholes is achieved using dowel pins. The outer radius of the central cylinder has an out-of-round error of less than $5\ \mu\text{m}$ and therefore is an exact reference to the center of the detector and the pinhole configurations. The central cylinder itself is placed into a medium fit which has been machined at both ends of the outer vacuum chamber. Onto the flanges at each end of the vacuum chamber four plane surfaces have been milled which act as reference marks with a defined distance to the center of the chamber within $30\ \mu\text{m}$.

A main issue of the design of the electronics housing is to allow on the one hand good pumping of the electronics in

¹following the German acronym "Röntgenlithographie Galvanik und Abformung"

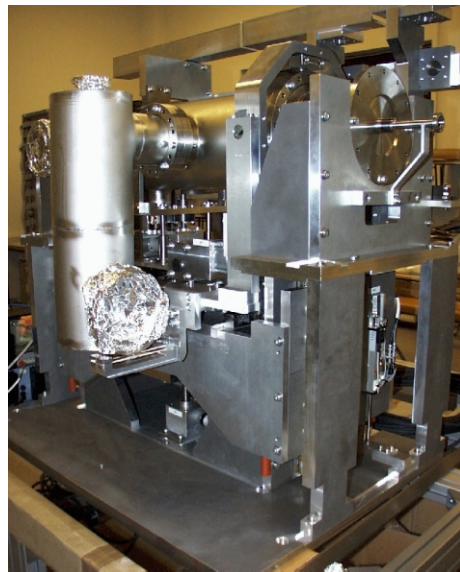


Figure 3: Vacuum chamber of the BTM prototype mounted onto its precise adjustment table.

order to reach ultra high vacuum conditions. On the other hand one had to separate it from the beam tube, because of the high induced electro-magnetic fields (wake fields) of the high charge ($\geq 1\ \text{nC}$) and ultra-short ($\leq 250\ \mu\text{m}$) bunches. It is therefore embedded into a shield of solid aluminum, which also serves as the mechanical support of the electronics. The pumping of the electronics components is done through suction slits into the central cylinder. To avoid the penetration of wake fields from the beam to the electronics a RF shield has been put around the cylinder. It consists of a fine mesh from $50\ \mu\text{m}$ thick wires out of stainless steel with holes of $100\ \mu\text{m}$.

Three different beam pipes are provided. The central beam pipe (inner diameter $7.5\ \text{mm}$) is surrounded by the detector chip and the pinhole mask. During operation of the BTM the silicon detectors are placed about $5\ \text{mm}$ away from the electron beam. To allow for the extraction of the silicon detectors during linac startup or beam adjustments from the immediate adjacency of the beam a dummy beam pipe (inner diameter $15\ \text{mm}$) is placed $53\ \text{mm}$ above the central one. Bellows on both sides of the vacuum chamber allow the necessary transverse movement.

2 TESTS OF THE PIXEL DETECTOR

2.1 Measurement of Spatial Accuracy

The detector is installed into the focal plane of a scanning electron microscope (SEM) [4]. The SEM produces an electron beam with an energy of $10\ \text{keV}$ focused to a spot smaller than $1\ \mu\text{m}$ on the surface of the detector. The electron beam is scanned across the two pixel rows in parallel to their separation line. After each scanning line, the electron beam is displaced by a fixed amount. The detector read-out is synchronized to the scanning frequency of the

SEM, so that data are taken after each scanned line. The zero crossing of the signal for the 12 pixel pairs scatters with a standard deviation of $0.47 \mu\text{m}$ around the symmetry line of the pixel detector.

2.2 Sensitivity to Vacuum Ultraviolet Radiation

We measured the sensitivity of the detector to vacuum ultraviolet (VUV) [4] at the synchrotron radiation facility HASYLAB. For this purpose the detector is illuminated with VUV radiation in the energy range between 50 eV and 1000 eV. The hybrid containing the silicon pixel detector and its read-out electronics is placed into the vacuum chamber of a reflectometer. The mono-energetic photon beam coming from the monochromator is focused onto the center of the pixel detector.

The silicon detector response was corrected to the photoelectron emission of one of the focusing mirrors and to a GaAs photo diode as a reference. The observed quantum efficiency is explained by the following effects: The electrical field of the detector diode does not extend up to the cathode plane, but leaves space for a dead layer with a thickness of the order of 30 nm, which has to be penetrated by the photons before they enter the sensitive region of the detector. A 50 nm thin passivation layer of silicon oxide on top of the back entrance window leads to further absorption of photons.

The quantum efficiency of the detector is larger than 20% for photons in the energy range above 100 eV which will be used by the BTM. Absolute measurements with a similar type of detector have been done using a reference diode with known quantum efficiency [3].

2.3 Study of Radiation Hardness

In the BTM the silicon detector will be operated at a distance of only 5 mm from the electron beam of the TTF linac. It can suffer from radiation damages caused by a beam halo or by scraping a misaligned beam. One expects that the radiation damages of the silicon detectors are dominated by surface effects.

Placing the silicon detector inside an electron microscope gives the opportunity to study radiation hardness against surface damages. One of the two pixel rows, including its JFETs, is irradiated using the 10 kV electron beam with beam currents of the order of several tens of pA. Irradiation takes place with all operating voltages on, including the bias voltage.

Measuring the detector noise one can clearly distinguish between the non-irradiated pixels and the irradiated ones. Whereas the first stayed at the same noise level the equivalent noise charge of the latter increased by a factor of three after a total radiation dose of 120 Gy. Above radiation doses of about 300 Gy some of the irradiated pixels cease to deliver any signal at all. The detector can cope with radiation doses up to 100 Gy. At the position of the BTM in TTF a radiation dose of the order of 1 Gy per week is expected.

2.4 Detector Calibration

Photons of 6 keV emitted by a ^{55}Fe source are used for the calibration of the four pixel detectors of the signal plane of the BTM prototype. The measured spectrum for pixel 12 ($100 \mu\text{m}$ wide) is shown in Fig. 4. It can be separated into three parts: The pedestal peak, which dominates the distribution, the signal peak, which consists of the K_{α} and K_{β} components, and the region in between, which is caused by charge sharing between adjacent pixels. Between pedestal and signal peak the diffusion region is visible. The energy scale, the noise and the diffusion width are determined with a simultaneous fit to the whole spectrum of Fig. 4 based on a model describing the two-dimensional pixel structure.

The width of the pedestal peak corresponds to an equivalent noise charge of 110 electrons. The difference between the signal and pedestal peak gives an energy calibration for each pixel. The relative difference between left and right pixels is below 5% for all pixel pairs. This results in an error of the position reconstruction of $0.4 \mu\text{m}$ for a $30 \mu\text{m}$ beam spot.

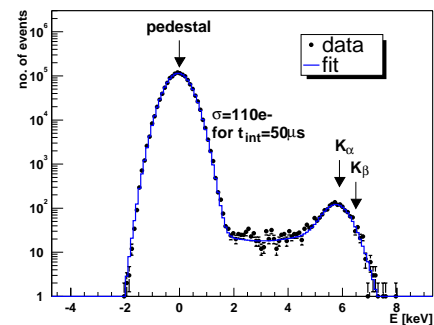


Figure 4: Measured energy spectrum of ^{55}Fe source.

3 OUTLOOK

All components are prepared and ready for the assembly of the BTM prototype. The installation into the TTF beam line and first beam measurements are planned for the second half of this year.

REFERENCES

- [1] TTF-FEL Conceptual Design Report, TESLA-FEL 95-03, DESY, June 1995; J. Rossbach *et al.*, Nucl. Instr. and Meth. **A375** (1996) 269.
- [2] J. S. T. Ng, TESLA-FEL 96-16, DESY, 1996; J. S. T. Ng *et al.*, Nucl. Instr. and Meth. **A439** (2000) 601.
- [3] P. Lechner, L. Strüder, Nucl. Instr. and Meth. **A354** (1995) 464; R. Hartmann *et al.*, Nucl. Instr. and Meth. **A377** (1996) 191; H. Soltau *et al.*, Nucl. Instr. and Meth. **A377** (1996) 340.
- [4] S. Hillert *et al.*, "Test Results on the Silicon Pixel Detector for the TTF-FEL Beam Trajectory Monitor", DESY 00-065, submitted to Nucl. Instr. and Meth. A.